WIND TUNNEL STUDIES OF

CIRCULATION CONTROL ELLIPTICAL AIRFOILS

M. E. Franke and J. K. Harvell
Air Force Institute of Technology

SUMMARY

Effects of blown jets on the lift and drag of cambered elliptical airfoils are described. Performance changes due to a splitter plate attached to the lower surface of an elliptical airfoil near the trailing edge with and without blowing are indicated. Lift and drag characteristics of airfoils with two blown jets are compared with airfoils with single blowing jets. Airfoil designs that vary the location of a second jet relative to a fixed jet are described.

INTRODUCTION

Numerous studies have demonstrated the basic concepts of circulation control airfoils (refs. 1 to 13). These studies have been supplemented by flight tests which have demonstrated further the application of circulation control lifting surfaces (refs. 14 to 16). A review paper has summarized circulation control technology (ref. 17).

Several areas that have not been studied extensively include the use of splitter plates and multiple-jet blowing in the airfoil trailing-edge region. The objective of this paper is to describe experimental studies that have been conducted to determine the low-speed lift and drag characteristics of circulation control elliptical airfoils using splitter plates and multiple jet blowing in the trailing-edge region. The paper will describe the effects of a number of parameters on the lift coefficient and the drag coefficient. These parameters include number of blown jets, locations of the blowing slots, splitter plate, splitter plate configuration, trailing-edge contour, airfoil angle of attack, and combinations of the above.

SYMBOLS

b	splitter plate chord
c	airfoil chord
c_d	section drag coefficient
c_{d_e}	equivalent drag coefficient

C_{d_f} equivalent force drag coefficient

C_{d_o} corrected profile drag coefficient

C_{d_r} profile (rake) drag coefficient

C_ℓ section lift coefficient

C_μ section momentum coefficient, $\dot{m}V_j/q_\infty c$

C_{μ_c} cylindrical plenum momentum coefficient

C_{μ_m} main plenum momentum coefficient

C_{μ_s} second plenum momentum coefficient; also C_{μ_c}

C_{μ_T} total momentum coefficient, $C_{\mu_m} + C_{\mu_s}$ or $C_{\mu_m} + C_{\mu_c}$

h   slot height

$\dot{m}$ jet mass flow rate per unit span

q   dynamic pressure, $\rho V_\infty^2/2$

R_e Reynolds number, $\rho V_\infty c/\mu$

V   velocity

x   coordinate along chord

α geometric angle of attack

β splitter plate deflection angle from airfoil chord

δ slot 2 deflection angle from airfoil chord

θ slot jet angle relative to chord

μ viscosity

ρ density

ϕ cylinder slot 2 rotation angle

Subscripts

c   cylindrical plenum

j   jet

m   main plenum

s   second plenum

∞   freestream

AIRFOIL DESCRIPTIONS

Several different airfoil configurations were tested in this study. Schematics of the airfoil models are shown in figures 1 to 4. The experimental models were 20-percent-thick elliptical airfoils with cambers ranging from 5 to 8 1/2 per cent. The models had a span of 0.66 m, a chord of 0.51 m, and blowing slot heights of 0.5 mm.

The airfoil model shown in figure 1 contained a single plenum. Blowing air entered the plenum through a 3.8-cm-diam pipe and discharged through the blowing slot located at $x/c = 0.96$. An enlarged view of the trailing-edge region is shown in figure 2. The jet at the blowing slot was directed approximately parallel to the chord as shown in figure 2. Forty-eight pressure taps were used to measure the static pressure along the upper and lower surfaces of the airfoil. Forty-four of these taps were located at centerspan and four taps were located off centerspan to check the uniformity of the flow.

The model shown in figure 3 contained two separate plena and two blowing slots. Otherwise, the model was similar to that shown in figure 1. Two different trailing edge inserts were used to provide different jet exit directions ($\delta = 45$ deg or $\delta = 58$ deg) for the second slot. The third model (fig. 4) also contained two separate plena. The circular trailing-edge surface of the airfoil was formed by the surface of the circular cylinder. The cylinder was also used as the plenum for the second blowing jet. The second slot was formed in the cylinder as shown in the enlarged view in figure 4. The second slot location was varied by rotating the cylinder. The main plenum contained two screens and a foam block placed along the span that helped to provide a more uniform spanwise pressure distribution and, consequently, a more uniform jet velocity along the span. Three dead stop and three tensioning screws, spaced evenly along the span, were used to fix the slot height h at 0.5 mm. The location of the main plenum blowing slot was fixed at 94.5% chord. The second slot height was set and maintained at 0.5 mm by caps at the ends of the cylinder and by cross members held in place with screws. No screens or foam were used in the cylindrical plenum.

Sixty-seven static pressure taps were distributed along the centerspan of the model; 27 on the suction surface, 23 on the pressure surface, and 17 on the circular trailing edge. Three static pressure taps were located 0.15 m on each side of centerspan to monitor the two-dimensionality of the flow. Further details of the models are available (refs. 18 to 21).

TEST APPARATUS

Tests were conducted in the Air Force Institute of Technology 1.5-m-diam wind tunnel, which is an open-circuit tunnel with a maximum test speed of approximately 134 m/s. The tests were run at speeds ranging from approximately 25 to 30 m/s which is equivalent to a tunnel dynamic pressure of approximately 0.05 m of water. Four pitot-static tubes were used to measure the dynamic pressure. The Reynolds number varied between 7.3×10^5 and 10^6. The turbulence factor of the tunnel is 1.5, which accounts for the effect of the propeller, guide vanes, and tunnel wall vibrations.

Each model was installed in the wind tunnel with its span vertical and was supported at each end of the span. Two large wooden side panels were installed in the 1.5-m-diam circular test section to provide a more two- dimensional section that was 0.8 x 1.5 m. Adjustments to the side walls were made to provide uniform flow in the section. The two-dimensionality was further increased by using endplates -- 1.2-m-diam, 5-mm thick and beveled at the edges -- on both ends of the airfoil to reduce boundary layer and finite span effects. The combination of the plates and the wind tunnel walls formed the 0.66 x 1.5 m test section.

The air supplied to both plena was routed through the supports. A 12.7-mm-throat-diameter venturi meter, located in each air supply line, was used to measure the mass flow rate to each plenum. Static pressure readings were obtained at taps located at and immediately upstream of each venturi throat. The temperature was measured with a copper-constantan thermocouple located upstream of each venturi meter.

A wake survey rake placed horizontally across the tunnel and 1.5c to 1.9c behind the airfoil was used to measure the momentum deficit in the wake. Ninety-four total head tubes and six static tubes, distributed along the span of the rake, were used to measure the pressure in the airfoil wake.

Alcohol manometers were used to measure the static pressure on the airfoil suface. Mercury manometers were used to measure the pressure at the venturi meters, and water manometers were used to measure the total pressure in the main and cylindrical plena.

DATA REDUCTION AND PROCEDURE

The manometer data were recorded on film, digitized, and then used to calculate the section coefficients. The standard wind tunnel corrections suggested by Pope (ref. 22) for solid blockage, wake blockage, and streamline curvature were applied to C_ℓ. Solid and wake blockage corrections were used also to adjust drag, freestream velocity, dynamic pressure, and Reynolds number.

The blowing jet momentum coefficient was defined in the usual manner as indicated in the list of symbols. When two blowing slots were used, a

total momentum coefficient was defined as the sum of the main plenum and second plenum momentum coefficients:

$$C_{\mu_T} = C_{\mu_m} + C_{\mu_s} \tag{1}$$

where $C_{\mu_s} = C_{\mu_c}$ for the cylindrical plenum.

The section lift coefficient C_ℓ was calculated from the pressure distribution on the airfoil surface. The section corrected profile drag coefficient was obtained from the profile (rake) coefficient based on the momentum deficit methods of Betz and Jones (ref. 23) and then corrected for the blowing slot jet flow that did not originate upstream of the airfoil, i.e.,

$$C_{d_o} = C_{d_r} - C_\mu \frac{V_\infty}{V_j} \tag{2}$$

where V_j was the calculated jet velocity in the jet exit plane based on isentropic expansion from plenum total pressure to freestream static pressure. The jet exit velocity actually depends, however, on the local static pressure at the slot exit. For two blowing slots

$$C_{d_o} = C_{d_r} - C_{\mu_m} \frac{V_\infty}{V_{j_m}} - C_{\mu_s} \frac{V_\infty}{V_{j_s}} \tag{3}$$

where $V_{j_s} = V_{j_c}$ for the cylindrical plenum. To facilitate comparison of circulation control airfoil performance with that of conventional airfoils, C_{d_o} was modified following Englar et al. (refs. 3 to 6) by the addition of dimensionless terms to account for energy expenditure to produce the blowing air flow and a ram drag effect. This results in an equivalent drag coefficient, which was defined in this study for two blowing slots as

$$C_{d_e} = C_{d_o} + C_{\mu_m} \left(\frac{V_{j_m}}{2V_\infty} + \frac{V_\infty}{V_{j_m}} \right) + C_{\mu_s} \left(\frac{V_{j_s}}{2V_\infty} + \frac{V_\infty}{V_{j_s}} \right) \tag{4}$$

Englar et al. (ref. 10) also defined an equivalent force drag coefficient. For this study the equivalent force drag coefficient was defined as

$$C_{d_f} = C_{d_o} + C_{\mu_m} + C_{\mu_s} \tag{5}$$

It is important to note before proceeding that sometimes corrections to C_{d_r} can be an order of magnitude larger than the actual measured drag. Thus, the effect of calculating C_μ based on expansion to freestream or to local static pressure can introduce variations in C_{d_e} or C_{d_f} of 25% or more. To be consistent with the lift results of others, C_μ was based on expansion to freestream pressure.

A second problem is that pointed out by Pope (ref. 22) that the wake rake, when used with the momentum deficit method, is only accurate when measuring drag on an airfoil that is not stalled. There are other considerations as well. One is that a wake rake, used in conjunction with a manometer bank, is a time-averaging device and readings of a cyclic behavior may be affected by the response time of the system. Another is that drag results have been reported in numerous ways in the literature and care must be taken when comparing results from different sources. Also, the penalties applied to the profile drag for energy expenditure and ram drag may not be approproate in all cases.

RESULTS AND DISCUSSION

Typical results showing the effects of a splitter plate, blowing slots, training-edge contour, angle of attack and various combinations are shown in figures 5 to 16. The effect of splitter plate chord for the x/c = 0.99 and β = 45 deg splitter plate configuration is shown in figure 5. The results indicate that the lift coefficient increased as the splitter plate chord was increased. The effect of angle of attack was as expected. Some separation occurred at positive angles of attack.

The effects of blowing (in terms of C_μ), splitter plate angle, and splitter plate location on C_ℓ and C_{d_f} are shown in figures 6 and 7, respectively. The lift coefficient generally increased with increases in C_μ for the range of C_μ considered and was higher for splitter plate angles of 45 and 60 deg then for a 30 deg angle. Compared with a clean airfoil, the splitter plate caused an increase in C_{d_f} of the airfoil at the lower values of C_μ considered. At the higher values of C_μ, C_{d_f} either increased or decreased relative to that of a clean airfoil depending on the splitter plate location and angle. Further results and details on the effects of a splitter plate on airfoil lift and drag are given by Stevenson et al. (ref. 18).

The results in figure 8, obtained by Oxford (ref. 19), show the effect of trailing-edge contour, slot position x/c, and slot angle θ on C_ℓ of an airfoil with a splitter plate. The variations were found to have little effect on C_ℓ over the range of C_μ shown in figure 8. The slot angle θ was the angle between the jet exit direction and the airfoil chord.

The use of two blowing jets was studied by Pajayakrit (ref. 20) using the airfoil model shown in figure 3. The lift coefficient and drag coefficient of the model (fig. 3) as a function of C_μ are shown in figures 9 and 10 for two different trailing-edge inserts. The results are for main plenum blowing only and are compared with the lift coefficient and drag

272

coefficient of airfoil (fig. 1) without a splitter plate. As shown in
figures 9 and 10, the curves for the two models differ somewhat but have
the same general trends. The curves for the same model (fig. 3) with the
different inserts indicate that slight differences in the installation in
the tunnel or in trailing-edge contour can cause differences in the
measurements. It was also found that nonuniformity in slot height led to a
nonuniform jet and reduced performance.

The effects of two-slot blowing on C_ℓ are shown in figure 11 for the
airfoil (fig. 3) with the 58-deg-jet-blowing insert. Main plenum
blowing alone was shown to be as effective as two-slot blowing over the
range and combinations of C_{μ_T} studied. Results (not shown) with the 45-
deg-jet-blowing insert showed that this configuration was less effective in
increasing C_ℓ than with δ = 58 deg. Plots of C_ℓ vs C_{d_f} are shown in
figures 12 and 13 for second-slot blowing angles δ of 58 deg and 45 deg,
respectively. The results with δ = 58 deg, figure 12, indicate that C_{df}
was somewhat less with two-slot blowing compared with C_{d_f} for main plenum
blowing alone at a given C_ℓ. For δ = 45 deg, C_{df} was higher at a given C_ℓ
for two-slot blowing compared with that for main plenum blowing alone,
figure 13.

The model shown in figure 4 was designed so that the location of a
second slot could be varied relative to a fixed, main-blowing slot. Tests
showed that the spanwise pressure and velocity distributions were uniform
within a few precent and that there was good flow attachment around the
trailing edge. Separation normally occurred at angles ranging from ϕ = 70
to 90 deg with blowing only from the main slot. Tests were run with the
second slot located at ϕ = 73 and 83 deg.

The lift coefficient as a function of total momentum coefficient C_{μ_T}
is shown in figure 14 for ϕ = 73 deg. The baseline curve with blowing
only from the main plenum (C_{μ_C} = 0) is also shown as a reference. In the
tests with two-slot blowing, C_{μ_m} was held constant (within $\pm$ 0.002), while
the blowing rate from the cylindrical plenum was varied. The value of C_{μ_m}
for each curve is identified in figure 14. The curves illustrate the
advantage of two-slot blowing over single-slot blowing. For example, at C_{μ_T}
= 0.05 there was up to a 50% increase in C_ℓ for two-slot blowing depending
on the value of C_{μ_m}. The results indicate that once the main plenum
blowing was sufficient to keep the boundary layer attached up to the second
blowing slot, any additional main plenum blowing in terms of C_μ did not
increase lift as much as that for an equivalent incremental amount of
blowing (in terms of C_μ) from the second slot. When the value of C_{μ_m} was
below that required for boundary-layer attachment up to the second slot,
blowing from the second slot was slightly less effective than an equivalent
amount of C_μ based on single-slot main plenum blowing. This is illustrated
in figure 14 by comparing the C_{μ_m} = 0 and 0.007 curves with the baseline C_{μ_C}
= 0 curve. The tests with C_{μ_m} = 0 and 0.007 were terminated at C_{μ_T} = 0.015
and 0.05, respectively, due to an unexplained audible resonance experienced
at the next test condition for each case. The results for ϕ = 83 deg
(ref. 21) were similar to those for ϕ = 73 deg, except that the minimum
value of C_{μ_m} had to be increased to keep the flow attached up to the second

blowing slot.

The blown jet velocities at the slot exits were always less than sonic. Typical jet exit velocities for single-slot blowing alone at $C_{\mu_m} \simeq$ 0.9 were $V_{j_m} \simeq$ 190 m/s, whereas for two-slot blowing at $C_{\mu_T} \simeq$ 0.9, V_{j_m} and V_{j_c} were on the order of 140 m/s. Loth and Boasson (ref. 24) replotted data from Englar (ref. 25) and showed that, at constant slot height, ΔC_ℓ increases rather linearly with V_j/V_∞. The results with single-slot (main plenum) blowing in this study showed a somewhat similar relationship. Loth and Boasson (ref. 24) also determined that for single-slot blowing at constant C_μ, the maximum value of ΔC_ℓ will be obtained at a V_j/V_∞ value of approximately 4.6. However, at a given C_μ, there is only about a 10% variation in ΔC_ℓ over a range of V_j/V_∞ values between 2.5 and 12. Herein, V_j/V_∞ was varied over a range of approximately 2 to 7, and, consequently, for single-slot blowing at constant C_μ, less than a 10% variation in ΔC_ℓ would be expected. With two-slot blowing, however, larger increases in ΔC_ℓ at constant C_{μ_T} are shown in figure 14. Apparently, by reducing jet velocity and introducing a second blown jet, the momentum and energy of the two jets are used more effectively in increasing C_ℓ.

Typical equivalent drag results are shown in figure 15. With single-slot blowing, C_{d_e} was found to be slightly greater than that of the two-slot configurations at equivalent C_{μ_T}. Since lift as a function of C_{μ_T} was significantly enhanced with two-slot blowing, lift-to-drag ratios C_ℓ/C_{d_e} shown in figure 16 were higher for two-slot blowing than for single-slot blowing.

CONCLUDING REMARKS

A single blown jet was effective in increasing the lift coefficient of an elliptical airfoil as the momentum coefficient was increased. At the same total momentum coefficient C_{μ_T}, two blown jets were more effective than a single jet in some cases. The relative location of the two jets was found to be important. When using two slots, maximum C_ℓ/C_{d_e} was obtained by limiting the blowing from the primary slot to just the amount needed to ensure good flow attachment up to the secondary slot. However, too little blowing from the primary slot reduced the effectiveness of blowing from the second slot to being equivalent to or less than that for a single slot. A fixed splitter plate improved performance under most conditions. Splitter plate effectiveness depended on splitter plate chord, angle, and location. Trailing-edge contour did not influence lift as much in combination with a splitter plate as otherwise might be expected. Better performance was obtained with uniform slot height.

REFERENCES

1. Englar, R.J.: Experimental Investigation of the High Velocity Coanda Wall Jet Applied to Bluff Trailing Edge Circulation Control Airfoils. Naval Ship Research and Development Center, Bethesda, MD, NSRDC Rept. 4708, 1975.

2. Davidson, I.M.: Aerofoil Boundary-Layer Control System. British Patent 913754, 1960.

3. Kind, R.J. and Maull, D.J.: An Experimental Investigation of a Low-Speed Circulation-Controlled Aerofoil. The Aeronautical Quarterly, Vol. 19, May 1968, pp. 170-182.

4. Williams, R.M. and Howe, H.J.: Two-Dimensional Subsonic Wind Tunnel Tests on a 20-Percent Thick, 5-Percent Cambered Circulation Control Airfoil. Naval Ship Research and Development Center, Bethesda, MD, NSRDC Tech. Note AL-176, 1970.

5. Englar, R.J.: Two-Dimensional Subsonic Wind Tunnel Tests of Two 15-Percent Thick Circulation Control Airfoils. David Taylor Naval Ship Research and Development Center, Bethsda, MD, DTNSRDC Tech. Note AL-211, 1971.

6. Englar, R.J.: Two-Dimensional Subsonic Wind Tunnel Investigations of a Cambered 30-Percent Thick Circulation Control Airfoil. Naval Ship Research and Development Center, Bethesda, MD, NSRDC Tech. Note AL-201, 1972.

7. Englar, R.J.: Subsonic Two-Dimensional Wind Tunnel Investigations of the High Lift Capability of Circulation Control Wing Sections. David Taylor Naval Ship Research and Development Center, Bethesda, MD, DTNSRDC Tech. Rept. ASED-274, 1975.

8. Walters, R.E., Myer D.P., and Holt D.J.: Circulation Control by Steady and Pulsed Blowing for a Cambered Elliptical Airfoil. West Virginia University, Morgantown, WV, AD751045, Aerospace Engineering TR-32, 1972.

9. Englar, R.J.: Circulation Control for High Lift and Drag Generation on STOL Aircraft. Journal of Aircraft, Vol. 12, May 1975, pp. 457-463.

10. Englar, R.J. Williams, R.M.: Test Techniques for High-Lift, Two-Dimensional Airfoils with Boundary Layer and Circulation Control for Application to Rotary Wing Aircraft. Naval Ship Research and Development Center, Bethesda, MD, NSRDC Report 4645, 1975.

11. Abramson, J.: Two-Dimensional Subsonic Wind Tunnel Evaluation of a 20-Percent Thick Circulation Control Airfoil. David Taylor Naval Ship Research and Development Center, Bethesda, MD, DTNSRDC Rept. ASED-311, Code 1619, 1975.

12. Abramson, J.: Two-Dimensional Subsonic Wind Tunnel Evaluation of Two Related Cambered 15-Percent Thick Circulation Control Airfoils. David Taylor Naval Ship Research and Development Center, Bethesda, MD, DTNSRDC Rept. ASED-373, 1977.

13. Smith, R.V.: A Theoretical and Experimental Study of Circulation Control with Reference to Fixed Wing Applications. University of Southampton, United Kingdom, Research Paper 582, 1978.

14. Loth, J.L., Fanucci, J.B., and Roberts, S.C.: Flight Performance of a Circulation Controlled STOL Aircraft. _Journal of Aircraft_, Vol. 13, March 1976, pp. 169-173.

15. Englar, R.J.: Development of the A-6/Circulation Control Wing Flight Demonstrator Configuration. David Taylor Naval Ship Research and Development Center, Bethesda, MD, DTNSRDC Rept. ASED 79/01, 1979.

16. Nichols, J.H., Jr., Englar, R.J., Harris M.J., and Huson, G.G.: Experimental Development of an Advanced Circulation Control Wing System for Navy STOL Aircraft. AIAA Paper 81-0151, January 1981.

17. Wood, N. and Nielsen, J.: Circulation Control Airfoils Past, Present, Future. AIAA Paper 85-0204, AIAA 23rd Aerospace Sciences Meeting, Reno, NV, January 1985.

18. Stevenson, T.A., Franke, M.E., Rhynard, W.E., Jr., and Snyder, J.R.: Wind-Tunnel Study of a Circulation-Controlled Elliptical Airfoil. _Journal of Aircraft_, Vol. 14, September 1977, pp. 881-885.

19. Oxford, Vayl S.: A Wind Tunnel Study of the Effects of Trailing Edge Modifications on the Lift-Drag Ratio of a Circulation Controlled Airfoil. MS Thesis, GAE/AA/75D-16, Air Force Institute of Technology, Wright-Patterson AFB, OH, 1975.

20. Pajayakrit, Palanunt: A Wind Tunnel Study of the Effects of Lower Surface Blowing on the Lift, Drag, and Lift-to-Drag Ratio of a Circulation Control Elliptical Airfoil. MS Thesis, GAE/AA/79D-13, Air Force Institute of Technology, Wright-Patterson AFB, OH, 1980.

21. Harvell, J.K. and Franke, M.E.: Aerodynamic Characteristics of a Circulation Control Elliptical Airfoil with Two Blown Jets. _Journal of Aircraft_, Vol. 22, No. 9, September 1985, pp. 737-742.

22. Pope, A.: _Wind Tunnel Testing_. John Wiley and Sons, Inc., New York, 1954.

23. Schlichting, H.: _Boundary Layer Theory_. 7th Ed., McGraw-Hill Book Co., New York, 1979.

24. Loth, J.L. and Boasson, M.: Circulation Controlled STOL Wing Optimization. _Journal of Aircraft_, Vol. 21, February 1984, pp. 128-134.

25. Englar, R.J.: Low-Speed Aerodynamic Characteristics of a Small Fixed Trailing-Edge Circulation Control Wing Configuration Fitted to a Supercritical Airfoil. David Taylor Naval Ship Research and Development Center, Bethesda, MD, DTNSRDC Rept. ASED-81/08, 1981.
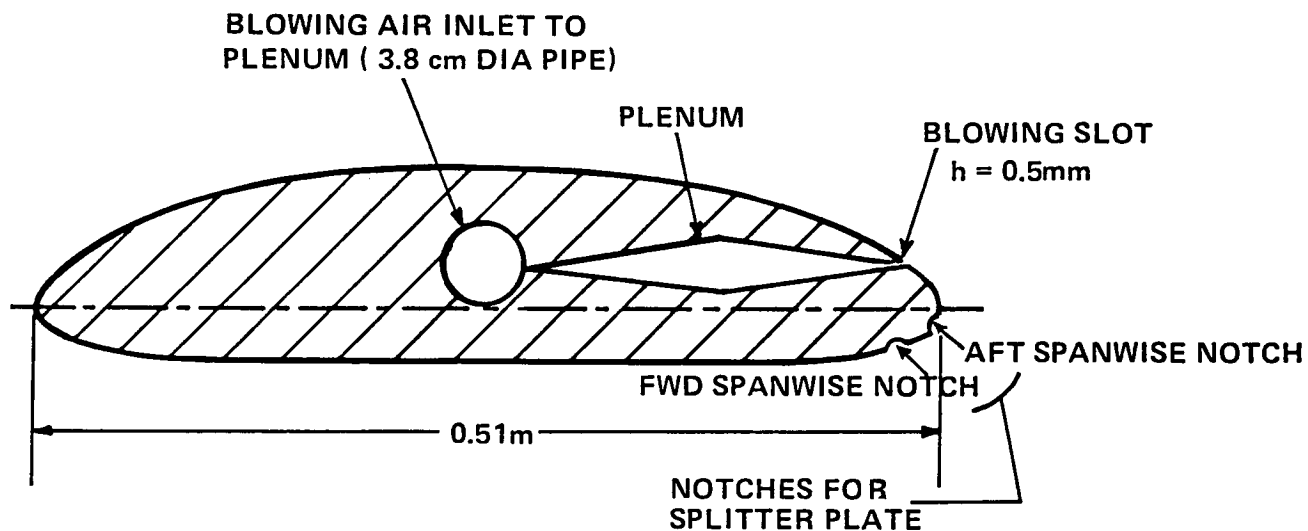
BLOWING AIR INLET TO PLENUM (3.8 cm DIA PIPE)

PLENUM

BLOWING SLOT
h = 0.5mm

AFT SPANWISE NOTCH

FWD SPANWISE NOTCH

0.51m

NOTCHES FOR SPLITTER PLATE

Figure 1. - Schematic of airfoil with single plenum.

BLOWING SLOT (x/c = 0.96)
(h = 0.5 mm)

SLOT ANGLE RELATIVE TO CHORD, Θ

TRAILING EDGE

X

SPLITTER PLATE POSITIONS

AFT NOTCH (x/c = 0.99)

β (VARIABLE 30, 45, or 60 deg)

FWD NOTCH (x/c = 0.95) FILLED WITH CLAY WHEN SPLITTER PLATE AT x/c = 0.99

SPLITTER PLATE CHORD b (VARIABLE 1.3, 2.5, or 3.8 cm)
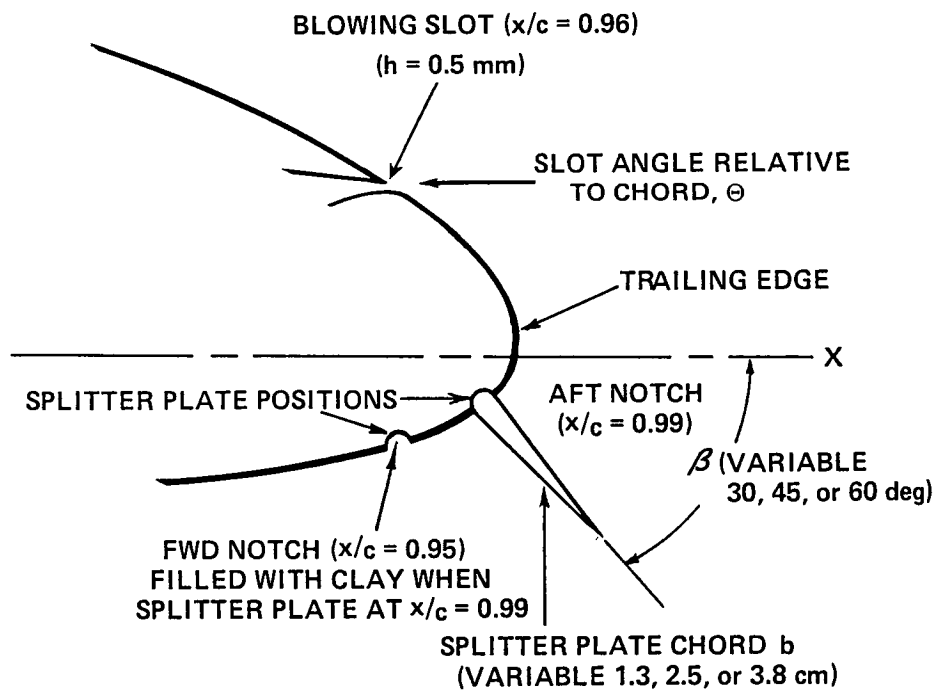
Figure 2. - Sketch of trailing edge with attached splitter plate.

C-4

BLOWING AIR INLETS
3.8 cm DIA PIPE

MAIN PLENUM
(NO. 1)

SLOT 1
x/c = 0.96
h = 0.5 mm

SECOND PLENUM (NO. 2)

0.51m

SLOT 2
x/c = 0.99
h = 0.5mm

REPLACEABLE
TRAILING EDGE
INSERT

ENLARGED VIEW
TRAILING EDGE INSERT

SLOT 2
x/c = 0.99
h = 0.5mm

δ
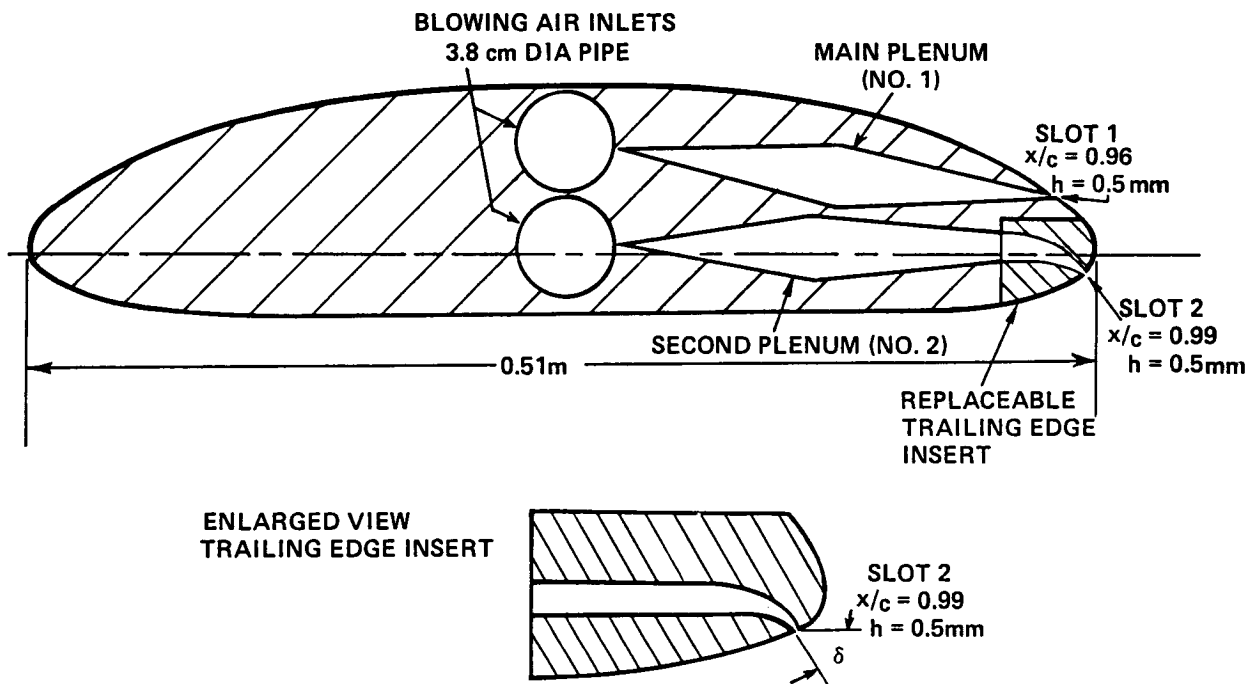
Figure 3. - Schematic of airfoil with two plena.

SCREEN

TENSION SCREWS
SUCTION SURFACE

φ

MAIN PLENUM INLET
MAIN PLENUM

FOAM FLOW
STRAIGHTENER
PRESSURE SURFACE

CYLINDRICAL
PLENUM

MAHOGANY
ALUMINUM
EPOXY

MAIN PLENUM

DEADSTOP &
TENSION SCREWS

SLOT 1
h = 0.5 mm
CYLINDRICAL PLENUM
(MOVABLE)
SLOT 2
h = 0.5 mm

CYLINDRICAL PLENUM
INLET
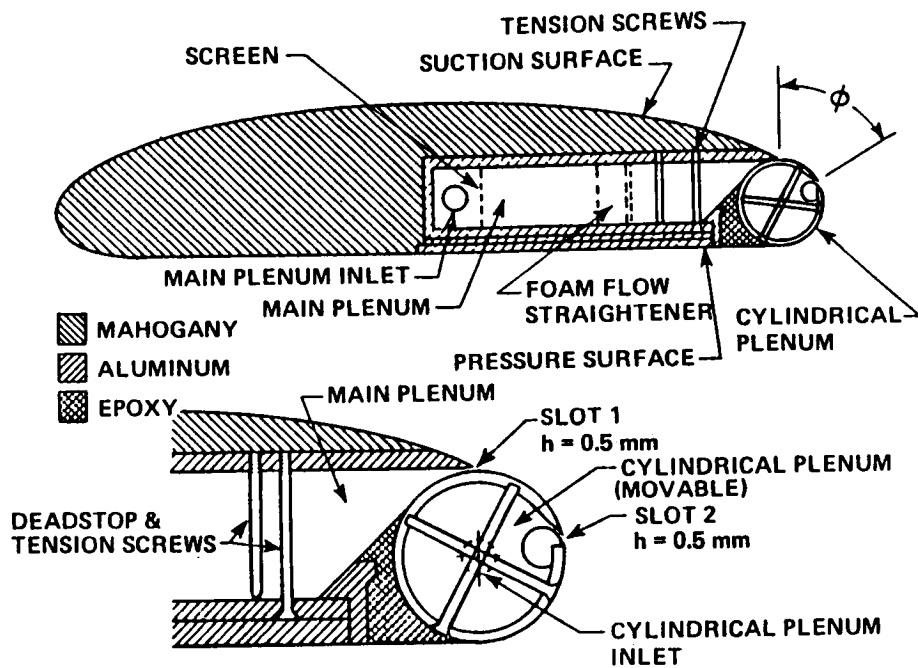
Figure 4. - Schematic of airfoil with two plena and rotatable circular
trailing edge.

278
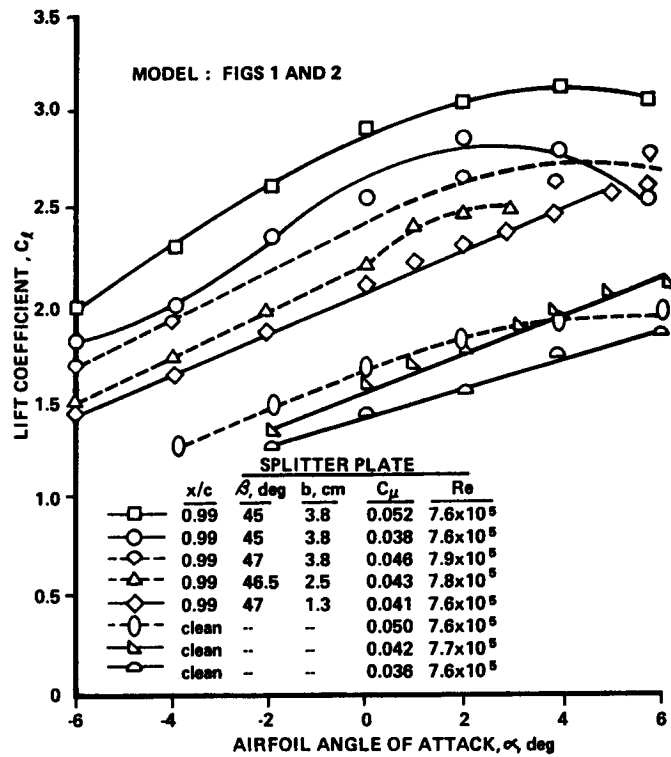
Figure 5. - Effect of blowing and splitter plate chord on lift coefficient.
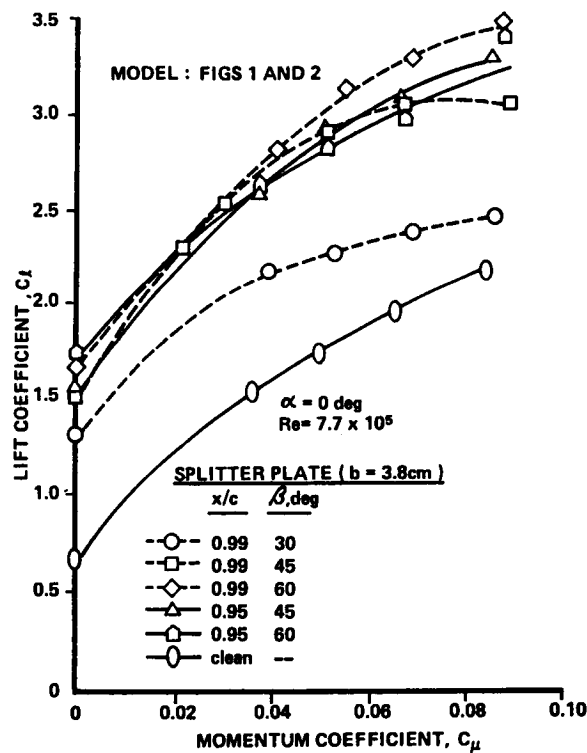
Figure 6. - Effect of blowing and splitter plate configuration on lift coefficient.

279
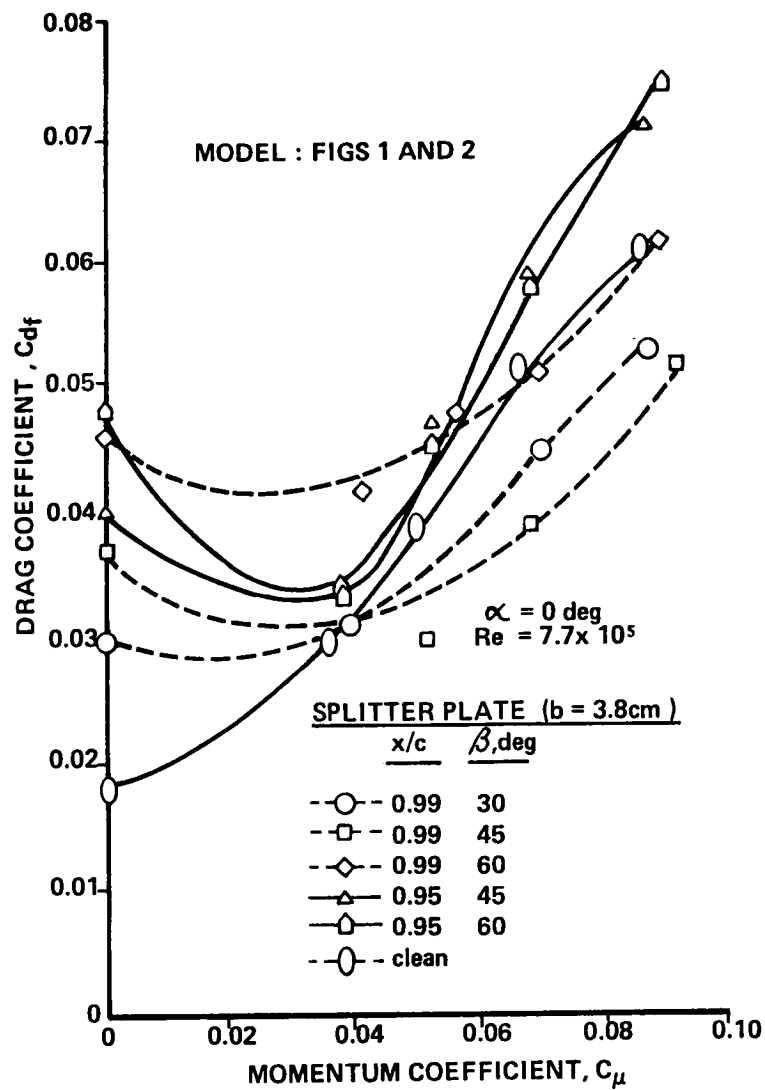
Figure 7. - Effect of blowing and splitter plate configuration on drag coefficient.

MODEL : FIGS 1 AND 2

LIFT COEFFICIENT, C_l

2.5

2.0

1.5

1.0

0.5

0

	TRAILING EDGE CONTOUR	SLOT POSITION x/c	SLOT ANGLE θ, deg
□	C	0.96	5
○	C	0.96	-33
◇	E	0.97	5
△	E	0.97	-33
◇	C	0.97	5
◯	C	0.97	-33

C - CIRCULAR
E - ELLIPTICAL

SPLITTER PLATE
b = 3.8 cm
β = 45 deg
x/c = 0.99

α = 0 deg
Re = 7.4x10⁵

0   0.01   0.02   0.03   0.04   0.05

MOMENTUM COEFFICIENT, C_μ
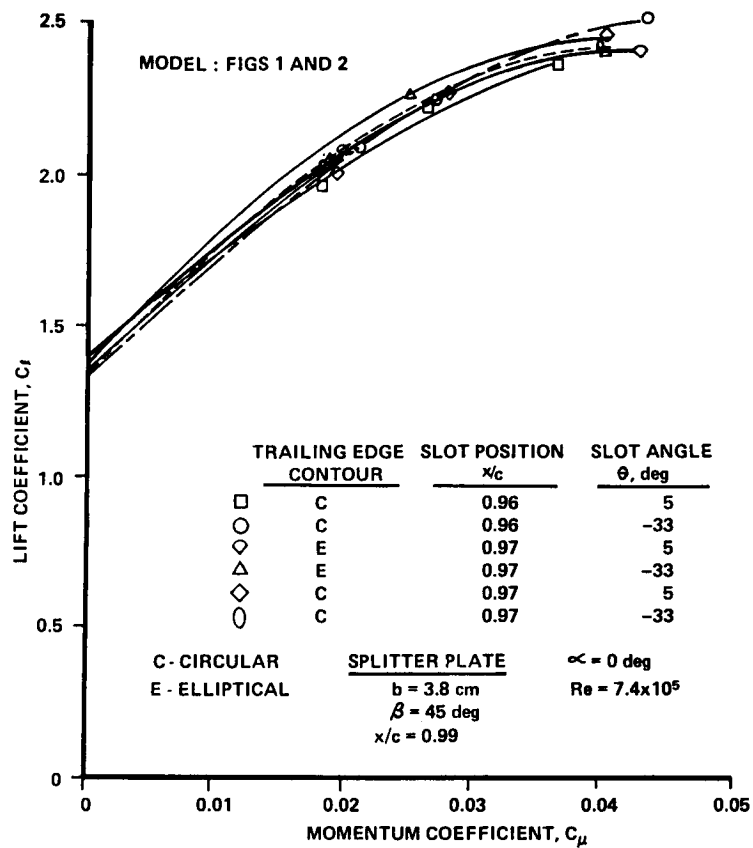
Figure 8. - Effect of trailing-edge configuration on lift coefficient with a splitter plate.

281
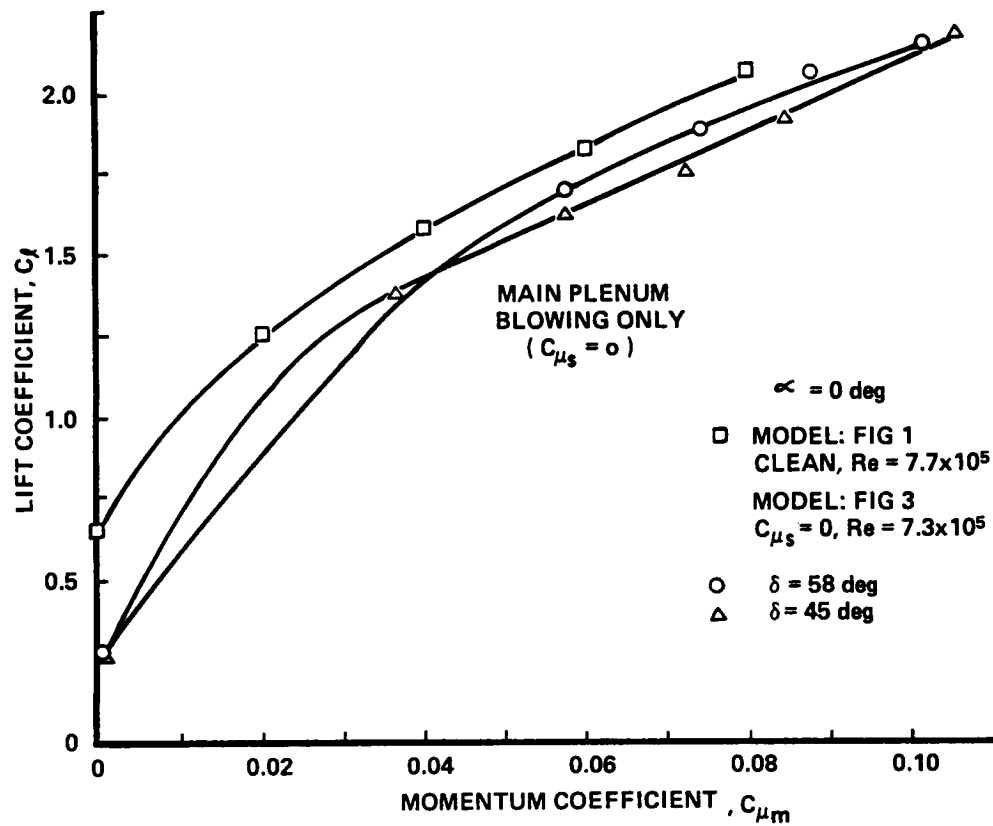
Figure 9. - Comparison of lift coefficient of airfoil (fig. 3) with that of airfoil (fig. 1).
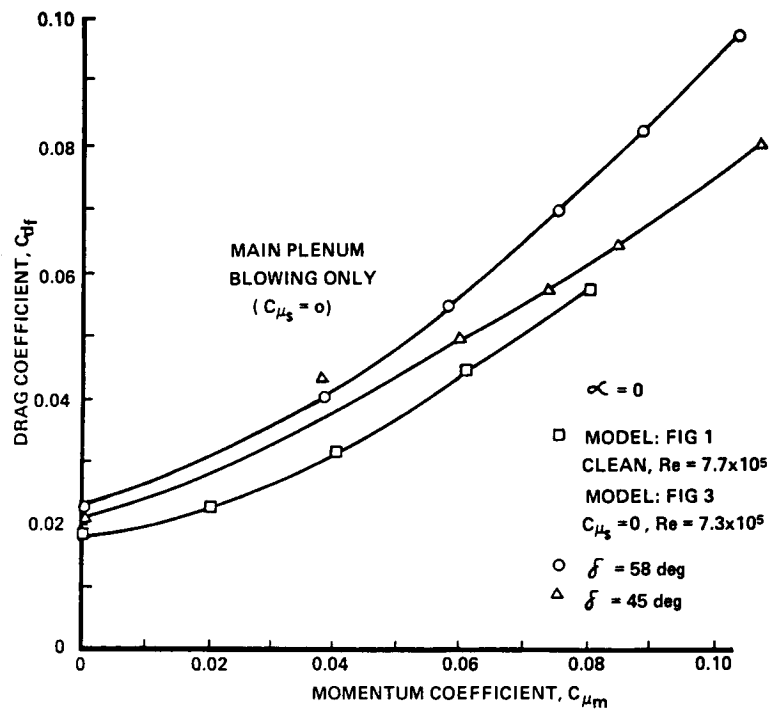
Figure 10. - Comparison of drag coefficient of airfoil (fig. 3) with that of airfoil (fig. 1).
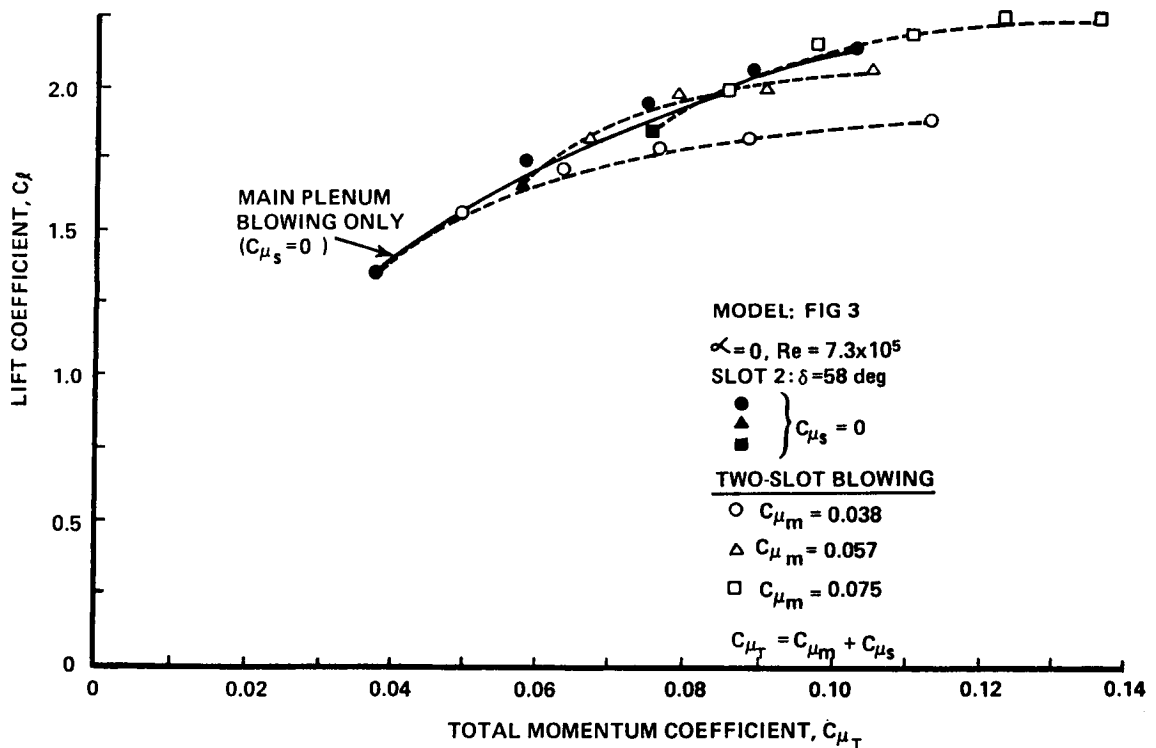
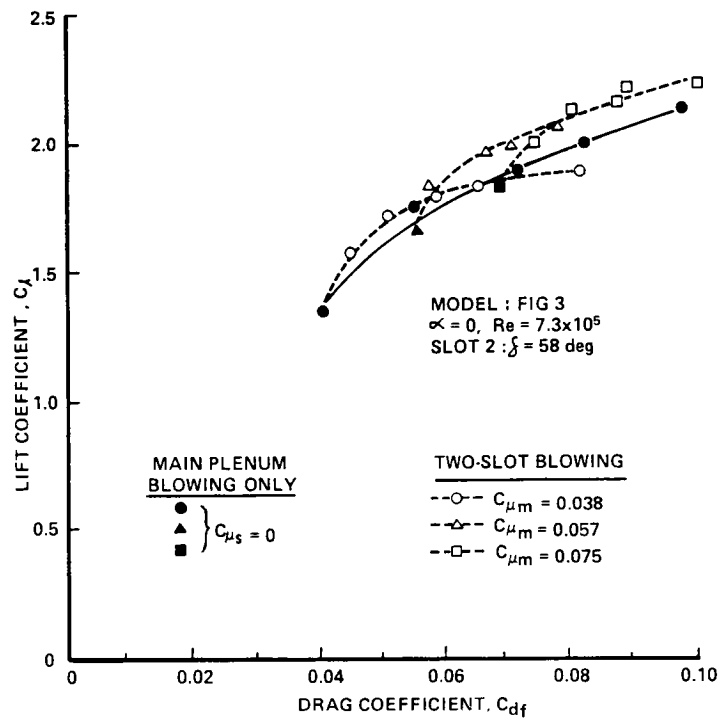Figure 11. - Effect of two-slot blowing on lift coefficient.

Figure 12. - Lift coefficient as a function of drag coefficient with blowing, δ = 58 deg.

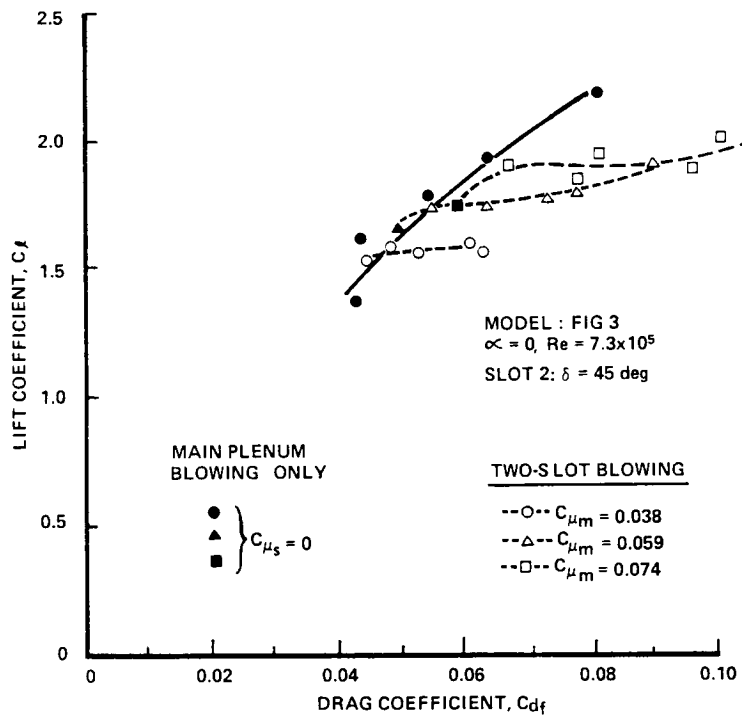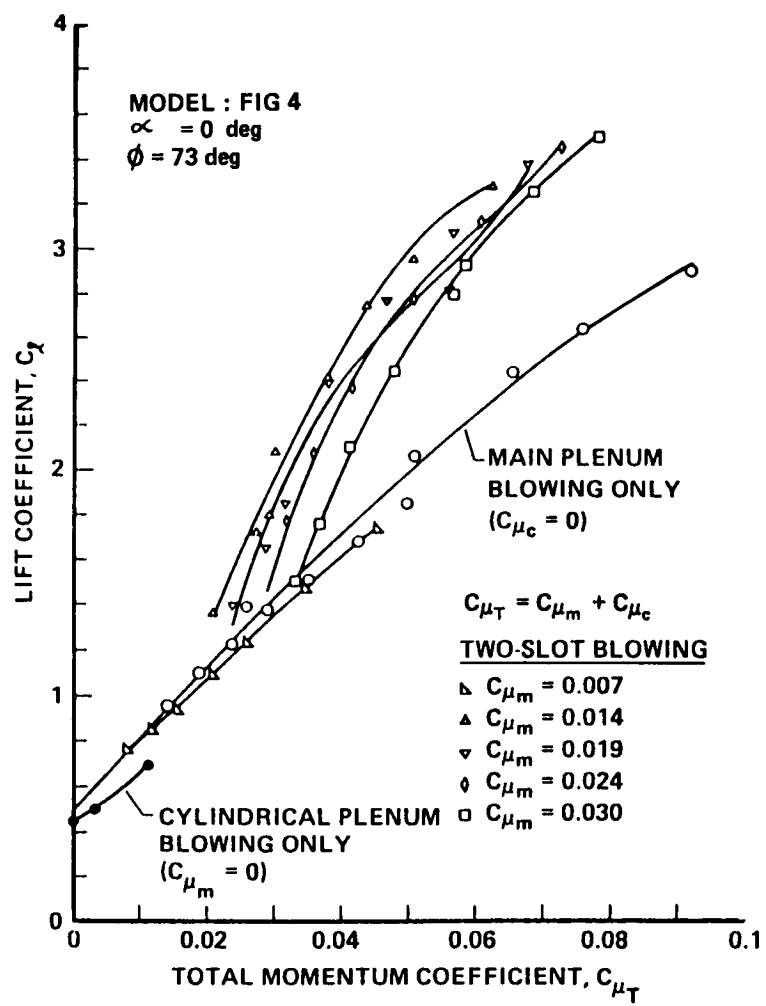Figure 13. - Lift coefficient as a function of drag coefficient with blowing, δ = 45 deg.

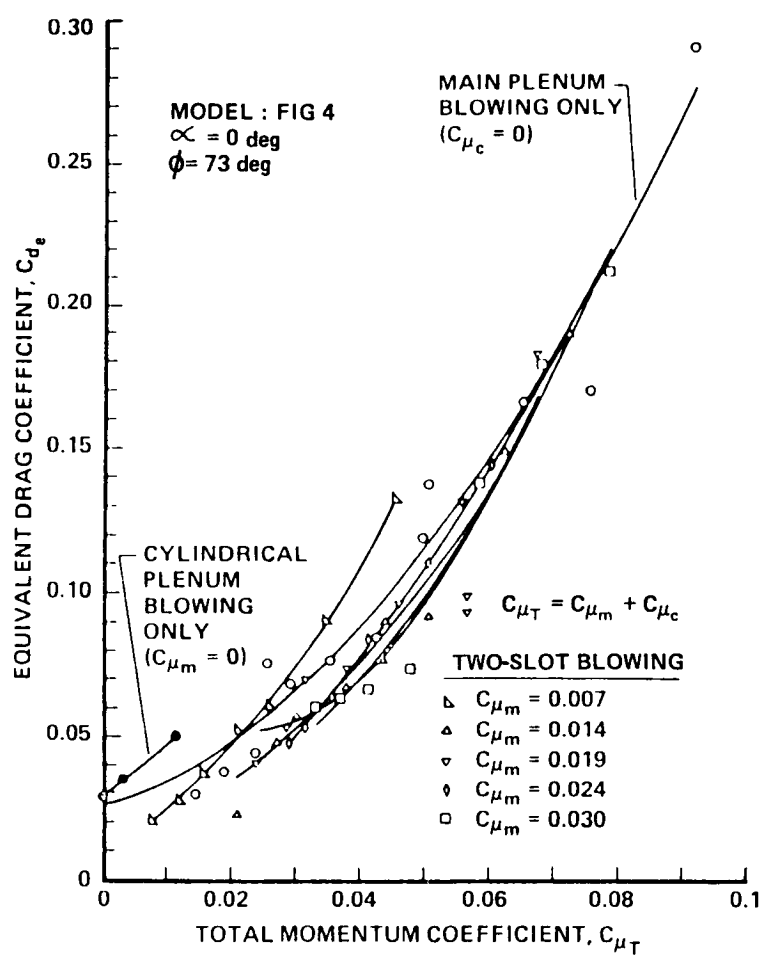Figure 14. - Effect of two-slot blowing on lift coefficient, ϕ = 73 deg.

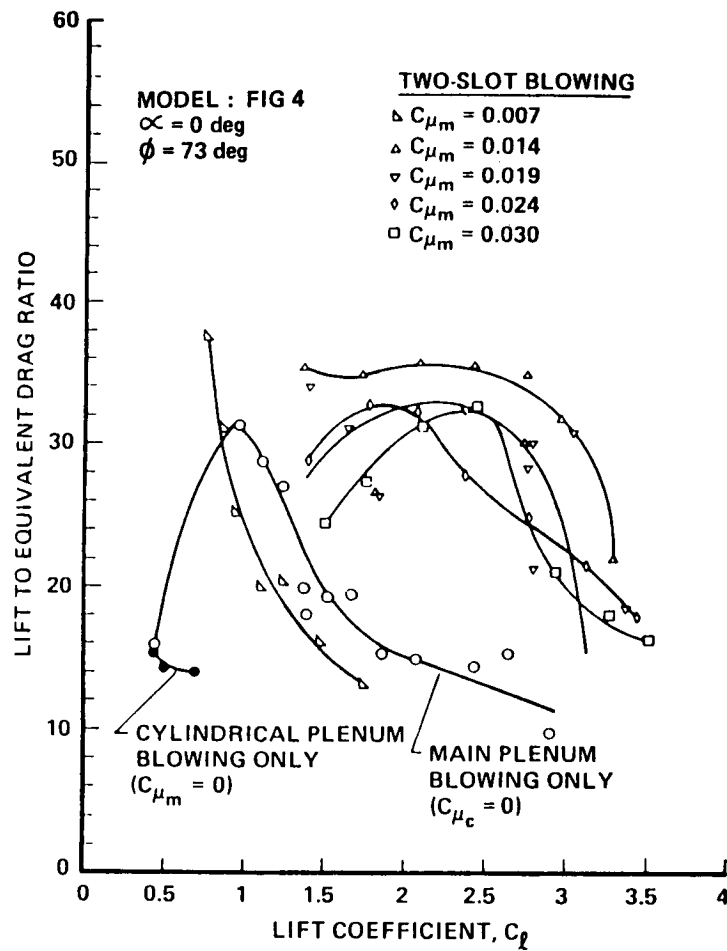Figure 15. - Effect of two-slot blowing on drag coefficient, ϕ = 73 deg.

Figure 16. - Lift-to-equivalent-drag ratio as a function of lift coefficient, ϕ = 73 deg.